DMD Fast Forward. Published on June 12, 2014 as DOI: 10.1124/dmd.114.058602
DMD Fast Forward. Published on June 12, 2014 as doi:10.1124/dmd.114.058602
This article has not been copyedited and formatted. The final version may differ from this version.

Evaluation of Calibration Curve-based Approaches to Predict Clinical Inducers and Non-inducers of CYP3A4 with plated human hepatocytes

J. George Zhang, Thuy Ho, Alanna L. Callendrello, Robert J. Clark, Elizabeth A. Santone, Sarah Kinsman, Deqing Xiao, Lisa G. Fox, Heidi J. Einolf and David M. Stresser

Corning Gentest Contract Research Services, Corning Life Sciences, Woburn, MA, USA (J.G.Z, T.H., A.L.C., R.J.C., E.A.S., S.K., D.X., L.G.F., D.M.S); Novartis Institutes for Biomedical Research, East Hanover, NJ, USA (H.J.E.)

Downloaded from dmd.aspetjournals.org at ASPET Journals on April 19, 2024

Copyright 2014 by the American Society for Pharmacology and Experimental Therapeutics.

DMD Fast Forward. Published on June 12, 2014 as DOI: 10.1124/dmd.114.058602
This article has not been copyedited and formatted. The final version may differ from this version.

Running Title: Prediction of CYP3A4 induction using Calibration Curves

Correspondence to: George Zhang, Ph.D., Corning Gentest Contract Research Services, Corning Life Sciences, 6 Henshaw Street, Woburn, MA. Phone: 781-938-2550; Email: zhangjg@corning.com

Text Pages: 21

Tables: 6

Figures: 8

References: 43

Abstract (words): 248

Introduction (words): 550

Discussion (words): 1500

Abbreviations: AUC, area under curve; CI, confidence interval; $C_{max\text{-}t}$, total systemic plasma concentration; $C_{max\text{-}u}$, unbound systemic plasma concentration; CYP, cytochrome P450; DDI, drug-drug interaction; EC_{50}, the concentration achieving 50% of the maximum response; EMA, European Medicines Agency; E_{max}, the maximum response; E_{min}, baseline of the dose-response curve; FDA, Food and Drug Administration; F_2, the concentration causing 2-fold increase from baseline of the dose-response curve; $f_{m,\ CYP3A}$, fraction metabolized, CYP3A; GMFE; geometric mean fold error; PBPK, physiologically-based pharmacokinetic models; PC, positive control; R^2, correlation coefficient; R_3, a term indicating the amount of CYP induction in the liver, expressed as a ratio between 0 and 1; RMSE, root mean square error; RIS, relative induction score; RT-PCR, real-time, reverse transcription polymerase chain reaction

Downloaded from dmd.aspetjournals.org at ASPET Journals on April 19, 2024

DMD Fast Forward. Published on June 12, 2014 as DOI: 10.1124/dmd.114.058602
This article has not been copyedited and formatted. The final version may differ from this version.

ABSTRACT

Cytochrome P450 (CYP) induction is often considered a liability in drug development. Using calibration curve-based approaches, we assessed the induction parameters R_3, relative induction score (RIS), C_{max}/EC_{50} and AUC/F_2, derived from concentration-response curves of CYP3A4 mRNA and enzyme activity data *in vitro*, as predictors of CYP3A4 induction potential *in vivo*. Plated cryopreserved human hepatocytes from three donors were treated with 20 test compounds, including several clinical inducers and non-inducers of CYP3A4. After the two day treatment, CYP3A4 mRNA levels and testosterone 6ß-hydroxylase activity were determined by RT-PCR and LC-MS/MS analysis, respectively. Our results demonstrated a strong and predictive relationship between the extent of midazolam AUC change in human and the various parameters calculated from both CYP3A4 mRNA and enzyme activity. The relationships exhibited with non-midazolam *in vivo* probes, in aggregate, were unsatisfactory. In general, the models yielded better fits when unbound rather than total plasma C_{max} was used to calculate the induction parameters, as evidenced by higher R^2 and lower RMSE and GMFE. With midazolam, the R_3 cut-off value of 0.9, as suggested by FDA guidance, effectively categorized strong inducers, but was less effective in classifying mid-range or weak inducers. This study supports the use of calibration curves generated from *in vitro* mRNA induction response curves to predict CYP3A4 induction potential in human. With the caveat that most compounds evaluated here were not strong inhibitors of enzyme activity, testosterone 6ß-hydroxylase activity was also demonstrated to be a strong predictor of CYP3A4 induction potential in this assay model.

Downloaded from dmd.aspetjournals.org at ASPET Journals on April 19, 2024

DMD Fast Forward. Published on June 12, 2014 as DOI: 10.1124/dmd.114.058602
This article has not been copyedited and formatted. The final version may differ from this version.

Introduction

The potential for new drug candidates to exhibit drug-drug interactions (DDI) is a significant concern during the drug development process. Because metabolism by cytochrome P450 enzymes (CYP) is often a major elimination pathway, small-molecule drug candidates are evaluated for CYP inhibition or induction at various stages of development. CYP3A4 comprises 15% to 30% of hepatic P450 content (Shimada et al. 1994; Ohtsuki et al, 2012) and is estimated to account for about half of oxidations in drugs undergoing P450-mediated clearance (Wienkers and Heath, 2005). Therefore, this enzyme is critical to evaluate as a mediator of DDI.

Prediction of human DDI based on *in vitro* data is another important goal during the early stages of drug development. Outcomes of these predictions may ultimately determine whether clinical DDI studies are conducted. Various models and frameworks have been proposed for induction prediction and these have been recently reviewed (Einolf et al. 2013; Almond et al. 2009; Fahmi and Ripp 2011). These include calibration curve-based approaches, mathematical or mechanistic static models, and physiologically-based pharmacokinetic (PBPK) models. Calibration curve-based models can be developed by comparing the observed clinical change in AUC of a probe substrate drug (such as midazolam for CYP3A4) for a set of known inducers/non-inducers of the enzyme of interest, with various *in vitro* induction potency parameters such as relative induction score (RIS) (Ripp et al. 2006), AUC/F_2 (Kanebratt and Andersson 2008), or C_{max}/EC_{50} (Fahmi and Ripp 2011) obtained from specific lots (donors) of cryopreserved hepatocytes. These models, as well as others (Kato et al. 2005; Shou et al. 2008, Fahmi et al. 2009), can be used to evaluate induction potential and risk of a clinical DDI. Recent guidance from the FDA (2012) and EMA (2013) suggest options for evaluating induction potential, ranging from simple, conservative

Downloaded from dmd.aspetjournals.org at ASPET Journals on April 19, 2024

DMD Fast Forward. Published on June 12, 2014 as DOI: 10.1124/dmd.114.058602
This article has not been copyedited and formatted. The final version may differ from this version.

models ("R_3" and a predefined fold-induction threshold) to more complex models as mentioned earlier (e.g. mechanistic static models, PBPK models, RIS). Both guidance documents advocate use of mRNA data, obtained using human hepatocytes. In addition, the documents generally recommend using donor lots that have been previously characterized with a sufficient number of clinical inducers and non-inducers (the EMA basic method being the exception).

Several *in vitro* test systems have been used for assessment and prediction of CYP3A4 induction potential in human by new drug candidates. These systems include primary cultures of cryopreserved human hepatocytes (McGinnity et al. 2009, Fahmi et al. 2010, Shou et al. 2008), human hepatocyte-like cell lines such as Fa2N-4 (Ripp et al. 2006; McGinnity et al. 2009), HepaRG (Kanebratt and Andersson 2008, McGinnity et al. 2009) and more recently a stably-expressed human PXR cell line derived from HepG2 (Fahmi et al. 2012). To date, human hepatocyte cultures have been considered the gold standard for *in vitro* induction assessment and are currently "preferred" by regulatory agencies.

The present work describes a direct comparison of several induction parameters (RIS, R_3, C_{max}/EC_{50}, and AUC/F_2) generated with a set of clinical inducers and non-inducers using human hepatocytes as *in vitro* system, to predict the *in vivo* CYP3A4 induction potential using a calibration curve. In this approach, calibration curves were constructed by plotting various parameters versus the change in clinical probe AUC of observed *in vivo*. The evaluations were conducted using endpoints of mRNA and testosterone 6ß-hydroxylase activity generated using either total or unbound plasma C_{max} in the models.

Downloaded from dmd.aspetjournals.org at ASPET Journals on April 19, 2024

DMD Fast Forward. Published on June 12, 2014 as DOI: 10.1124/dmd.114.058602
This article has not been copyedited and formatted. The final version may differ from this version.

Materials and Methods

Materials and Reagents. A set of twenty compounds comprised primarily of clinical inducers and non-inducers were evaluated *in vitro* at concentrations selected based on previous publications (Ripp et al., 2006; Kanebratt and Andersson 2008; McGinnity et al., 2009; Fahmi et al., 2010) (Table 1) and experience within this laboratory. Dimethyl sulfoxide (DMSO), testosterone, acetonitrile, ethanol, and all test drugs were purchased from Sigma-Aldrich (St. Louis, MO) and were of the highest grade available. Inducible cryopreserved human hepatocytes, Corning® hepatocyte culture medium, 6β-hydroxytestosterone, 6β-hydroxytestosterone-[D_7], Corning® high viability cryohepatocyte recovery kits, and collagen type I-coated 96-well plates were obtained from Corning Life Science (Tewksbury, MA). Gentamicin was obtained from Lonza (Walkersville, MD). Fungizone®, L-glutamine and D-phosphate buffered saline were from Gibco (Grand Island, NY). The RNeasy 96 kit and DNase I were from Qiagen (Valencia, CA). Reverse transcription kit, two-step TaqMan® PCR Master Reaction Mix, primers/probes were obtained from Applied Biosystems (Foster City, CA).

Human Hepatocyte Culture and Treatment. Inducible cryopreserved human hepatocytes (Lots 295, 312, and 318) were rapidly thawed and plated at a density of 0.6 x 10^6 viable cells/mL (100 µL/well) in collagen type-I-coated 96-well plates using high viability cryohepatocyte recovery kits. After approximately 4 hours, the plating medium was replaced with 100 µL of hepatocyte culture medium supplemented with 2 mM L-glutamine, 50 µg/mL gentamicin, and 0.75 µg/mL fungizone, and the cultures were maintained overnight. Hepatocyte cultures were treated for two days with 0.1% DMSO (negative control) and test drugs at eight concentrations each except for primaquine, methotrexate, and digoxin, for which three or four concentrations

Downloaded from dmd.aspetjournals.org at ASPET Journals on April 19, 2024

DMD Fast Forward. Published on June 12, 2014 as DOI: 10.1124/dmd.114.058602
This article has not been copyedited and formatted. The final version may differ from this version.

were tested. All incubations were performed in triplicate. The test concentration range is shown in Table 2.

***In Situ* CYP3A4 Activity Measurement.** The testosterone 6ß-hydroxylase activity assay was performed essentially as described by Zhang et al (2010). Briefly, after treatment, hepatocyte cultures were washed with culture medium and incubated with 100 µL of culture medium containing CYP3A4 probe substrate testosterone at a concentration of 200 µM for 30 min. The reactions were stopped by combining an aliquot from each well with acetonitrile containing internal standard 6β-hydroxytestosterone-[D_7]. The amount of metabolite formed was determined by LC-MS/MS using an API-4000 mass spectrometer. The culture plates were stored at - 80 ºC until total RNA isolation.

Determination of Test Drug Concentrations in Incubation Medium. At the end of the second day of treatment, the incubation medium from lot 295 was collected and combined with acetonitrile containing internal standard labetalol. The relative concentrations of test drug remaining in the incubation medium were quantitated by LC-MS/MS using an API-4000 mass spectrometer.

Total RNA Isolation and Real-time Reverse Transcription Polymerase Chain Reaction (RT-PCR) Analysis. Total RNA was isolated from cells using the RNeasy® 96 kit according to instructions provided by the manufacturer. The mRNA expression for CYP3A4 and the house keeping gene β-actin was determined by Taqman® RT-PCR methods using the two-step assay protocol. First, a reverse transcription (RT) assay was performed using a GeneAmp® PCR System 9700 (Applied Biosystems) with equal volume of total RNA and the RT master mixture. For the PCR assay, a PCR master mixture of reagents was prepared and a 20 µL aliquot of the

Downloaded from dmd.aspetjournals.org at ASPET Journals on April 19, 2024

DMD Fast Forward. Published on June 12, 2014 as DOI: 10.1124/dmd.114.058602
This article has not been copyedited and formatted. The final version may differ from this version.

master mixture was transferred to a 96-well optical reaction plate, followed by the addition of 5 μL of acquired *c*DNA to the appropriate wells. The PCR amplification was performed and the transcription was determined using an ABI 7300 Real Time PCR System.

Data Calculation. The test drug concentrations (μM) remaining in the incubation medium after the two day treatment and the catalytic activity for CYP3A4 in hepatocytes were calculated using standard curves. The fold induction for activity data was calculated as follows: (enzyme activity of test drug)/(mean of enzyme activity of negative control). The fold induction for mRNA data was determined using the calculation of $2^{-\Delta\Delta CT}$ (Livak and Schmittgen, 2001). Percentage of positive control response for both activity and mRNA was calculated as follows: (mean of observed maximal fold-1)/(mean of observed maximal fold by rifampicin-1).

Curve Fitting. To estimate EC_{50}, E_{max}, and F_2 values, concentration-response fold induction data were fitted to a Sigmoid dose-response one site fit model (4 Parameter Logistic Model; Model 205) with XLfit™ (ID Business Solutions, Emeryville, CA) according to equation 1:

$$Induction\ response(fold) = E_{\min} + \left(\frac{E_{\max} - E_{\min}}{1 + (\frac{EC_{50}}{C})^{d}} \right) \quad (1)$$

where E_{min} is the baseline of the curve, E_{max} is the maximum effect, EC_{50} is the concentration achieving 50% of E_{max}, d is the slope of the curve, and C is the drug concentration. An additional parameter, F_2, which is the drug concentration that causes a 2-fold increase of E_{min} was also calculated. The curve fitting was conducted using the following acceptance criteria and conditions: 1) data points were excluded from curve fitting when toxicity, insolubility, and inhibition (enzyme activity only) were apparent or when the coefficient of variation of replicate

Downloaded from dmd.aspetjournals.org at ASPET Journals on April 19, 2024

DMD Fast Forward. Published on June 12, 2014 as DOI: 10.1124/dmd.114.058602
This article has not been copyedited and formatted. The final version may differ from this version.

values was >40% after removing the offending outlier in the original set of triplicate samples); 2) curve fitting data were not used when R^2 of the fit was <0.85; 3) when no apparent plateau was observed after the above mentioned conditions were taken into consideration, the E_{max} was constrained to the observed maximal fold to prevent extrapolation of the curve fit beyond measured data, and EC_{50} was then obtained from the fitted curves. 4) EC_{50} and E_{max} were determined only when fold induction was at least 1.4-fold and the response was concentration-dependent.

The RIS and "R_3" values were calculated according to equations 2 and 3, according to the EMA (2013) and FDA (2012) guidance documents, respectively.

$$RIS = \frac{E_{\max} \times [I]}{EC_{50} + [I]} \quad (2)$$

$$R_3 = \frac{1}{\left(\frac{1 + d \times E_{\max} \times [I]}{(EC_{50} + [I])}\right)} \quad (3)$$

Where [I] is total or unbound systemic plasma C_{max}, d is a scaling factor assumed to be 1 (FDA draft guidance, 2012). Although R_3 as defined in FDA guidance does not permit use of unbound C_{max} as the value of [I], as part of our investigation, we elected to examine the effect of both total and unbound C_{max} on model outcomes.

The C_{max} (total and unbound)/EC_{50} and AUC/F_2 were also calculated, where AUC is the *in vivo* exposure of the interacting drug, represented by the area under the plasma concentration over time course (Table 3).

Downloaded from dmd.aspetjournals.org at ASPET Journals on April 19, 2024

DMD Fast Forward. Published on June 12, 2014 as DOI: 10.1124/dmd.114.058602
This article has not been copyedited and formatted. The final version may differ from this version.

Preparation of Calibration Curves. A set of nine clinical inducers and clinical non-inducers with known midazolam AUC changes after single dosing and clinical pharmacokinetic data was used for the preparation of calibration curves. The compounds included three strong inducers: rifampicin (with four clinical study data points), phenytoin, and carbamazepine; four moderate/weak inducers: troglitazone, terbinafine, pleconaril, and pioglitazone; and two clinical non- inducers nifedipine and clotrimazole (Table 3, as indicated with asterisks). Flumazenil was excluded from the calibration curves because very weak induction was observed in only one of the three donors (mRNA only) and it's extremely low C_{max} would have yielded a data point far removed from the range of the other points on the calibration curve. The remaining interacting drugs examined here were not used to generate the calibration curves. This is because we used only those compounds where associated clinical data was obtained with the well-established CYP3A4 probe midazolam as the victim drug (see Table 3). *In vitro* data generated for those compounds with non-midazolam clinical data were then evaluated against the curve generated with the aforementioned nine compounds. The calibration curves were constructed with the observed midazolam AUC change against calculated induction parameters (RIS, R_3, C_{max}/EC_{50} and AUC/F_2) using equation 4:

$$\%\ AUC\ change = A + \left(\frac{B - A}{1 + (\frac{C}{x})^d} \right) \qquad (4)$$

where A is the baseline of the curve constrained to 0%; B is the maximum AUC change constrained to ≤ 100%, C is the values of induction parameters "x" (RIS, R_3, C_{max}/EC_{50} and AUC/F_2) achieving 50% of AUC change and *d* is the slope of the curve. The cut-off values for a

Downloaded from dmd.aspetjournals.org at ASPET Journals on April 19, 2024

DMD Fast Forward. Published on June 12, 2014 as DOI: 10.1124/dmd.114.058602
This article has not been copyedited and formatted. The final version may differ from this version.

positive inducer were defined as the induction parameter values leading to a 20% decrease in predicted midazolam AUC change (FDA 2012). The analysis included determination of the 95% confidence interval (CI) for the cut-off values (95% probability that the predicted cut-off values will occur) and correlation coefficient (R^2) for goodness of fit. Statistical parameters were determined using the Statistics Designer function with XLfit™ software.

Comparison of model predictability. To compare the prediction accuracy of each model, the root mean square error (RMSE) was calculated as described in equation (5), with greater accuracy being shown by the lower RMSE. The fold changes of predicted DDI and the observed DDI were calculated as $AUC_{induced}/AUC_{control}$. The bias of the prediction models was determined by the geometric mean fold error (GMFE) in equation (6), which weighs over- and under-predictions equally. The lowest GMFE value would represent the lowest prediction bias.

$$\text{RMSE} = \sqrt{\frac{\sum(\text{predicted DDI} - \text{observed DDI})^2}{\text{number of predictions}}} \quad (5)$$

$$\text{GMFE} = 10^{\frac{\sum\left|\log\left(\frac{\text{predicted DDI}}{\text{observed DDI}}\right)\right|}{\text{number of predictions}}} \quad (6)$$

Downloaded from dmd.aspetjournals.org at ASPET Journals on April 19, 2024

DMD Fast Forward. Published on June 12, 2014 as DOI: 10.1124/dmd.114.058602
This article has not been copyedited and formatted. The final version may differ from this version.

Results

Concentration-dependent Induction Response of CYP3A4 mRNA and Activity in Human Hepatocytes. Hepatocytes from lots 295 (aged 41, female and Caucasian), 312 (aged 56, male and Caucasian) and 318 (aged 58, male and African American) were treated for two days with a medium change and compound replenishment after 24 hours. Both CYP3A4 mRNA levels and catalytic activities were measured. The parameters EC_{50}, E_{max}, and F_2 were determined from the concentration-response curves and % of positive control response was also determined. Overall, EC_{50} values obtained from both CYP3A4 mRNA and enzyme activity were similar (e.g. within 3-fold) within and between donors, with some notable exceptions (Tables 1 and 2). For example, EC_{50} for rifampicin was 0.12 and 0.18 for mRNA and enzyme activity, respectively for lot 295, but was 1.4 µM and 1.1 µM for same endpoints respectively for lot 312. E_{max} values obtained from mRNA data, in general were greater than those from the activity results. The weak clinical inducers sulfinpyrazone and probenecid produced a potent induction response of CYP3A4 mRNA and/or activity and the response did not reach plateau at the highest concentration within any of the lots (data not shown). Flumazenil caused no induction for both mRNA and activity in lots 295 and 318, however, a slight induction response for CYP3A4 mRNA was observed in lot 312 at the high end of the concentration-response curve. As expected, most compounds previously shown to be inducers *in vivo* and *in vitro* caused a greater than 2-fold induction over vehicle control and exhibited concentration-dependence, the criteria to demonstrate a positive

Downloaded from dmd.aspetjournals.org at ASPET Journals on April 19, 2024

DMD Fast Forward. Published on June 12, 2014 as DOI: 10.1124/dmd.114.058602
This article has not been copyedited and formatted. The final version may differ from this version.

induction result as described in the EMA guidance (2013). A few moderate and/or weak clinical inducers failed to reach these cut-off values for either mRNA or activity for some of these three lots of hepatocytes, such as pleconaril and pioglitazone. Quinidine at the concentration range of 0.11-250 μM caused an induction of CYP3A4 mRNA in two of the 3 lots, but not for enzyme activity for all lots. No induction of CYP3A4 mRNA and activity was observed for primaquine, methotrexate, and digoxin at the concentrations tested in any of the three lots.

Comparison of Calibration Curves for RIS, R_3, C_{max}/EC_{50}, and AUC/F_2. To examine the relationship between induction data generated *in vitro* and data observed in clinical studies (Tables 3), the RIS, R_3, and C_{max}/EC_{50} values were calculated based on both total and unbound C_{max} (Supplemental Tables 1-3, Table 5). The calibration curves were then prepared with the % observed AUC changes of midazolam as a function of parameters RIS, R_3, C_{max}/EC_{50}, and AUC/F_2 as shown in Figures 1-4 (see Supplemental Figures 1-8 for lots 312 and 318). The proposed cut-off values corresponding to a 20% of predicted midazolam AUC change *in vivo*, 95% confidence interval for the cut-off values, and correlation coefficient R^2 for the calibration curves are summarized in Table 4. Overall, excellent correlation between the induction parameters and observed midazolam AUC changes was obtained with the choice of model with reasonable 95% confidence intervals and R^2 values (0.84-0.995 for mRNA and 0.78-0.99 for activity). Cut-off values were within 3-fold for both mRNA and activity across all three lots for RIS, R_3, and C_{max}/EC_{50}. Relative to other parameters, the cut-off values for AUC/F_2 appeared to vary more across all three lots of hepatocytes.

Assessment of R_3 Cut-off Value in Prediction of CYP3A4 Inducers. The R_3 values for each interacting drug were calculated based on both total and unbound C_{max} and are presented in Table

Downloaded from dmd.aspetjournals.org at ASPET Journals on April 19, 2024

DMD Fast Forward. Published on June 12, 2014 as DOI: 10.1124/dmd.114.058602
This article has not been copyedited and formatted. The final version may differ from this version.

5. These values were compared with 0.9, a cut-off value for a likely inducer *in vivo* as proposed in the FDA draft guidance (2012). As shown in Table 5, R_3 values calculated with both C_{max-t} and C_{max-u} classified the strong clinical inducers well, but were less accurate in categorizing mid-range or weak inducers. For example, using C_{max-t} , the calculated R_3 values for some of clinical non-inducers such as nifedipine, rosiglitazone, omeprazole, and quinidine were <0.9, resulting in false positive assignments. In contrast, R_3 values calculated based on C_{max-u} were >0.9 for some moderate and weak inducers such as troglitazone, terbinafine, pleconaril and pioglitazone, leading to false negative assignments. This was true of all 3 donors regardless of using mRNA or activity as the endpoint.

Predicted AUC Changes using the Calibration Curves. Using the constructed calibration curves, the AUC changes for 16 interacting drugs were predicted from all three lots and compared with the observed AUC changes (Figures 5-7, Supplemental Tables 4-7). As expected, the predicted AUC changes were close to fitted values for the nine interacting drugs with midazolam as the victim drug, although a slight over-prediction was observed for troglitazone and terbinafine using RIS and R_3, calculated based on C_{max-t} (both activity and mRNA) in some of these lots. The correlation plots between the observed and predicted midazolam AUC changes for three hepatocyte lots were prepared for all induction parameters (Figures 5-7). As anticipated, a strong correlation (R^2 = 0.85-0.97) for both mRNA and activity was obtained with the observed AUC changes, regardless of the parameters used. No obvious difference in the robustness of the prediction in midazolam AUC changes was observed using the mRNA versus the activity data. The prediction accuracy and bias for each model were analyzed by RMSE and GMFE using a set of data from both three lots and a single lot. Table 6 shows similar GMFE and RMSE values calculated from this set of three lots for the different prediction methods

Downloaded from dmd.aspetjournals.org at ASPET Journals on April 19, 2024

DMD Fast Forward. Published on June 12, 2014 as DOI: 10.1124/dmd.114.058602
This article has not been copyedited and formatted. The final version may differ from this version.

using mRNA or activity as the measured end point. RMSE and GMFE analysis from a single lot provided similar results (data not shown). We found that the correlation was largely improved for all parameters (RIS, R_3, and C_{max}/EC_{50}) for both mRNA and activity (R^2 >0.94) when using C_{max-u}. Consistent with these observations, lower RMSE and GMFE values were obtained when using C_{max-u} instead of C_{max-t} in the prediction methods (Table 6). No apparent correlation was observed between the observed midazolam or non-midazolam AUC changes and % of positive control response for both activity and mRNA for all three lots (R^2 =0.13-0.41) (Figure 8).

The prediction for the interacting drugs with non-midazolam victim drugs was also conducted with these calibration curves. Weak correlations between the observed and predicted non-midazolam AUC changes for three hepatocyte lots for all induction parameters were found (Figures 5-7) (R^2 <0.40). However, parameters predicted clinical non-inducers reasonably well except for quinidine where a significant over-prediction (32%-93% midazolam AUC change) was found using RIS, R_3, and C_{max}/EC_{50}, generated from mRNA data based on C_{max-u} for lot 295 and 312. However, no induction was predicted with AUC/F_2 from both mRNA and activity data for quinidine across all three lots. For moderate/weak inducers, the AUC change for non-midazolam drugs was predicted with varied accuracy. In general, the prediction accuracy was lower and bias was greater in the prediction of the AUC change of CYP3A substrates that were not midazolam. This is evident in the lower RMSE and GMFE values for midazolam trials, as shown in Table 6. In a few cases, either over- or under-prediction was also observed for the *in vivo* AUC changes of nifedipine by phenobarbital, alprazolam by carbamazepine, simvastatin by troglitazone and pioglitazone, depending on parameters and hepatocyte lots (Supplemental Tables 4-7). Significant over-prediction was consistently found for the AUC changes of R-warfarin by sulfinpyrazone (22% observed AUC change vs 59%-94% predicted midazolam

Downloaded from dmd.aspetjournals.org at ASPET Journals on April 19, 2024

DMD Fast Forward. Published on June 12, 2014 as DOI: 10.1124/dmd.114.058602
This article has not been copyedited and formatted. The final version may differ from this version.

AUC change) and of carbamazepine by probenecid (20% observed AUC change versus 70%-94% predicted midazolam AUC change), with all parameters for both activity and mRNA across all lots except for AUC/F_2 for lot 318 (Supplemental Tables 4-7).

Concentration of test compounds in the medium. The results of such testing in the present study are shown in Supplemental Table 8 for lot 295. Within this set of compounds, concentrations ranged from close to nominal to well below nominal.

Downloaded from dmd.aspetjournals.org at ASPET Journals on April 19, 2024

DMD Fast Forward. Published on June 12, 2014 as DOI: 10.1124/dmd.114.058602
This article has not been copyedited and formatted. The final version may differ from this version.

Discussion

In this study, model compounds were evaluated for CYP3A4 induction in human hepatocytes and calibration curves constructed to predict responses *in vivo*. As expected, we observed notable inter-donor differences in EC_{50} and E_{max} values (e.g. rifampicin EC_{50} values), which supports regulatory agency guidance recommending calibration of hepatocyte donors for response with a set of inducers and non-inducers. Using resulting calibration curves, inducers were predicted with variable accuracy, whereas non-inducers were generally well-predicted.

Isolated false positive and false negative outcomes were observed. For example, phenobarbital was predicted as a non-inducer with the victim drug nifedipine when the calibration curves of total C_{max}/EC_{50} from the enzyme activity and/or mRNA data were used (lots 295 and 312). As phenobarbital is a clinical inducer, these results suggest evaluating multiple parameter endpoints would be conservative. Quinidine was also incorrectly classified as an *in vivo* inducer when mRNA was used as the predictor in the RIS, R_3, and C_{max}/EC_{50} calibration curve models obtained based on C_{max-u} with donors 295 and 312. This outcome was attributable to the concentration-dependent induction response of CYP3A4 mRNA, but not activity. Quinidine has been classified as a moderate CYP3A4 inhibitor *in vivo* (Isoherranen et. al. 2012) suggesting any induction *in vivo* could be masked. These data highlight the value of acquiring enzyme activity results to help one consider additional, more complex models. For example, the "net-effect" model (Fahmi et al, 2009) incorporates parameters of competitive and time-dependent inhibition that may provide a more informed prediction of clinical DDI.

Our data also suggest that midazolam calibration curves may over-predict AUC changes of non-midazolam victim drugs for weak/moderate inducers, as evidenced by higher midazolam AUC

Downloaded from dmd.aspetjournals.org at ASPET Journals on April 19, 2024

DMD Fast Forward. Published on June 12, 2014 as DOI: 10.1124/dmd.114.058602
This article has not been copyedited and formatted. The final version may differ from this version.

change compared to those obtained with other victim drugs. This is illustrated with predictions of alprazolam AUC change by carbamazepine and simvastatin AUC change by pioglitazone and troglitazone (Table 3, Supplemental Tables 4-7). Similarly, significant over-prediction of *in vivo* response using the midazolam curve was found for sulfinpyrazone and probenecid compared to the observed responses with victim drugs, R-warfarin and carbamazepine. This finding was consistent for all three hepatocytes lots with all modeled induction parameters with exception of AUC/F_2 for lot 318, regardless of activity or mRNA endpoint. Fahmi et al (2012) also reported an over-prediction for sulfinpyrazone using midazolam-RIS calibration curves in DPX2 cells. As midazolam exhibits a very high $f_{m,\ CYP3A}$, it is likely more susceptible to CYP3A4 induction than victim drugs (e.g. R-warfarin) cleared by additional pathways (Ripp et al. 2006; Xu et al. 2011). These findings underscore the use of midazolam as a preferential and sensitive clinical probe for DDI investigations. Notably, two clinically weak inducers, pioglitazone and pleconaril failed to always reach the 2-fold minimum induction response *in vitro* that would classify a compound as an inducer according to EMA guidance. However, this criterion was met for one or more of the other donors underscoring the value of using 3 donors in the standard test.

All calculated induction parameters incorporated *in vivo* total or unbound plasma concentrations of the interacting drugs. Regulatory guidance from the EMA (2013) and FDA (2012) recommend that C_{max-u} be used for RIS calculation and C_{max-t} for the R_3 calculation, respectively. Our results showed that the AUC changes were reasonably well-predicted when using either C_{max-t} or C_{max-u} to calculate parameters and was the case for both mRNA and enzyme activity. However, use of C_{max-u} resulted in a better correlation between observed and predicted midazolam AUC change (Figures 5-8) with an improved accuracy and precision of predicting the DDI, as RMSE and GMSE were lower (Table 6). These observations are consistent with a previous report (Ripp

Downloaded from dmd.aspetjournals.org at ASPET Journals on April 19, 2024

DMD Fast Forward. Published on June 12, 2014 as DOI: 10.1124/dmd.114.058602
This article has not been copyedited and formatted. The final version may differ from this version.

et al. 2006). Conversely, Fahmi et al (2012) demonstrated that use of total systemic drug concentration in a RIS evaluation resulted in significant improvement in DDI correlations in DPX2 cells, possibly attributable to inclusion of 10% serum in the incubation medium that likely affected the free-fraction in the medium.

The FDA draft guidance (2012) indicates that an investigational drug is likely to be a CYP inducer when the calculated R_3 value is below 0.9. We showed that R_3 cut-off values predicting a 20% midazolam AUC change (e.g. a DDI) were much lower than 0.9 (ranging from 0.44 to 0.65 for CYP3A4 mRNA as well as enzyme activity, across the three lots). Accordingly, we observed a relatively high rate of false positives (e.g. up to 50% exhibited $R_3 < 0.9$). When R_3 values were calculated using $C_{max\text{-}u}$, we found several false negative outcomes (Table 5). These data indicate that the 0.9 cut-off value along with the prescribed use of $C_{max\text{-}t}$ proposed by the FDA is conservative. In our evaluation we set the scaling factor "d" equal to 1 as this is the "assumed" value according to the guidance. Modifying the d value (or the R_3 cut-off value) may improve the accuracy of the classifications.

Both regulatory agency guidance documents recommend mRNA as the endpoint for testing induction potential. Fahmi et al (2010) showed that the measurement of CYP3A4 mRNA was more sensitive in detecting induction in hepatocytes compared to enzyme activity, while both endpoints were found effective at classifying clinical induction response. Our results support a similar conclusion. In general, we selected compounds in our test set biased away from potent inhibitors of CYP3A4 enzyme, to avoid the potentially confounding effects of enzyme inhibition. Clotrimazole, which was shown to exhibit a K_i value for liver microsomal CYP3A4 of 0.25 nM (Gibbs et al, 1999), is the notable exception. In this case, metabolic depletion and/or the wash

Downloaded from dmd.aspetjournals.org at ASPET Journals on April 19, 2024

DMD Fast Forward. Published on June 12, 2014 as DOI: 10.1124/dmd.114.058602
This article has not been copyedited and formatted. The final version may differ from this version.

steps conducted prior to testosterone addition likely precluded significant inhibition. Enzyme activity alone would probably have limited value as a predictor when examining compounds found to strongly or irreversibly inhibit enzyme activity within hepatocytes (e.g. ritonavir) as this may not always show a corresponding result *in vivo* (Kirby et al, 2011). Both midazolam (*in vivo* probe) and testosterone (*in vitro* probe) are substrates of CYP3A5 (Williams et al, 2003). This weakly inducible enzyme (Fahmi et al, 2010) exhibits polymorphic expression [(e.g. expressed in 10 to 30% of Caucasians and 50%-70% of African Americans (Daly, 2006)]. Whether clinical subject and hepatocyte donor CYP3A5 genotype status would help explain some variability in the models is not known.

Calculations of F_2, RIS, R_3, and C_{max}/EC_{50}, require preparation of a dose-response curve, ideally with sigmoidal shape and well-defined maxima and minima. While minima were reasonably well-defined, we noted that approximately 70% of compounds did not reach clear maxima, likely due to compound incomplete solubility, cytotoxicity, enzyme inhibition, or a combination thereof. In about 15% of the curves, a plateau was not reached because the concentration range was likely insufficient. For these cases, we deployed a strategy of constraining E_{max} to the observed maximal fold induction level that exhibited no evidence of insolubility or cytotoxicity; the EC_{50} parameter was then obtained from the curve fitting model. An alternative approach to not reaching well-defined maxima is to use the slope of the curve or AUC/F_2 as predictors (Shou et al. 2008; Kanebratt and Andersson, 2008). Our data support the value of obtaining the AUC/F_2 parameter.

In an *in vitro* induction assay, nominal and final (e.g. at the end of the treatment period), intracellular concentrations may differ and could impact model predictivity. Differences may be

Downloaded from dmd.aspetjournals.org at ASPET Journals on April 19, 2024

DMD Fast Forward. Published on June 12, 2014 as DOI: 10.1124/dmd.114.058602
This article has not been copyedited and formatted. The final version may differ from this version.

attributable to cellular uptake, metabolic depletion, compound degradation, binding to cellular components or the plate or a combination of these. As recommended by the EMA guidance, we investigated drug concentrations in the medium on the last day of incubation. For eleven out of seventeen compounds, concentrations were within approximately 2-fold of nominal at the concentrations closest to the reported C_{max-u}. However, six compounds exhibited concentrations < 20% of nominal (Supplemental Table 8), suggesting that intracellular unbound concentrations were substantially less than those used to derive EC_{50} and E_{max}. When we used the time-weighted average concentrations to derive these parameters, in general, EC_{50} values were lower and E_{max} values were unchanged. Somewhat surprisingly, this exercise showed no improvement on RMSE and GMFE for any parameter (results not shown).

In conclusion, *in vivo* CYP3A4 induction responses were well-predicted by the plated-hepatocyte model, using parameters RIS, R_3, C_{max}/EC_{50}, and AUC/F_2 in calibration-curve based models. Our data provide no strong basis for selecting a preferential model for predicting an induction response, although AUC/F_2 was somewhat less accurate and exhibited higher prediction bias. Enzyme activity and mRNA were equally effective as endpoints. If only one endpoint can be generated, mRNA is preferred, due to the potential confounding effects of enzyme inhibition. However, we found examples (e.g. quinidine) where integrating results of both mRNA and enzyme activity could provide a higher level of confidence in the evaluation as compared to either endpoint alone. In a general evaluation scheme the development stage, considering the resources needed to construct calibration curves as well as the potential need for range-finding, we would suggest using a 3-donor screening test to first classify a potential inducer from a basic method (such as described in the EMA guidance), followed by the more comprehensive RIS testing in calibrated hepatocytes for those compounds exhibiting induction.

Downloaded from dmd.aspetjournals.org at ASPET Journals on April 19, 2024

DMD Fast Forward. Published on June 12, 2014 as DOI: 10.1124/dmd.114.058602
This article has not been copyedited and formatted. The final version may differ from this version.

Acknowledgements

We thank Dr. Charles Crespi from Corning Life Sciences for reviewing the manuscript and for providing useful suggestions.

Authorship Contributions

Participated in Research design: Zhang and Stresser

Conducted experiments: Zhang, Ho, Callendrello, Clark, Santone, Xiao

Performed data analysis: Zhang, Stresser, Einolf, Kinsman

Wrote or contributed to the writing of the manuscript: Zhang, Stresser, Einolf, Fox

Downloaded from dmd.aspetjournals.org at ASPET Journals on April 19, 2024

DMD Fast Forward. Published on June 12, 2014 as DOI: 10.1124/dmd.114.058602
This article has not been copyedited and formatted. The final version may differ from this version.

References

Adams M, Pieniaszek HJ Jr, Gammaitoni AR and Ahdieh H (2005) Oxymorphone extended release does not affect CYP2C9 or CYP3A4 metabolic pathways. *J Clin Pharmacol* **45:**337-345.

Ahonen J, Olkkola KT and Neuvonen PJ (1995) Effect of itraconazole and terbinafine on the pharmacokinetics and pharmacodynamics of midazolam in healthy volunteers. *Br J Clin Pharmacol* **40:**270-272.

Almond LM, Yang J, Jamei M, Tucker GT, Rostami-Hodjegan A (2009) Towards a quantitative framework for the prediction of DDIs arising from cytochrome P450 induction. *Curr Drug Metab* **10:**420-432.

Backman JT, Olkkola KT and Neuvonen PJ (1996)[a] Rifampin drastically reduces plasma concentrations and effects of oral midazolam. *Clin Pharmacol Ther* **59:**7-13.

Backman JT, Olkkola KT, Ojala M, Laaksovirta H and Neuvonen PJ (1996) [b] Concentrations and effects of oral midazolam are greatly reduced in patients treated with carbamazepine or phenytoin. *Epilepsia* **37:**253-257.

Backman JT, Kivistö KT, Olkkola KT and Neuvonen PJ (1998) The area under the plasma concentration-time curve for oral midazolam is 400-fold larger during treatment with itraconazole than with rifampicin. *Eur J Clin Pharmacol* **54:**53-58.

Daly AK (2006) Significance of the minor cytochrome P450 3A isoforms. Clin Pharmacokinet **45**:13-31.

Eap CB, Buclin T, Cucchia G, Zullino D, Hustert E, Bleiber G, Golay KP, AubertAC, Baumann P, Telenti A and Kerb R (2004) Oral administration of a low dose of midazolam (75 microg) as an *in vivo* probefor CYP3A activity. *Eur J Clin Pharmacol* **60:2**37-246.

Downloaded from dmd.aspetjournals.org at ASPET Journals on April 19, 2024

DMD Fast Forward. Published on June 12, 2014 as DOI: 10.1124/dmd.114.058602
This article has not been copyedited and formatted. The final version may differ from this version.

Einolf HJ, Chen L, Fahmi OA, Gibson CR, Obach RS, Shebley M, Silva J, Sinz MW, Unadkat JD, Zhang L and Zhao P (2013) Evaluation of various static and dynamic modeling methods to predict clinical CYP3A induction using *in vitro* CYP3A4 mRNA induction data. C*lin Pharmacol Ther* doi: 10.1038/clpt.2013.170.

European Medicine Agency (EMA) (2013) Guideline on the investigation of drug interactions (final). http://www.ema.europa.eu/docs/en_GB/document_library/Scientific_guideline/2012/07/WC500129606.pdf.

Fahmi OA, Hurst S, Plowchalk D, Cook J, Guo F, Youdim K, Dickins M, Phipps A, Darekar A, Hyland R, Obach RS (2009) Comparison of different algorithms for predicting clinical drug-drug interactions, based on the use of CYP3A4 *in vitro* data: predictions of compounds as precipitants of interaction. *Drug Metab Dispos* **37:**1658-1666.

Fahmi OA, Kish M, Boldt S and Obach RS (2010) Cytochrome P450 3A4 mRNA is a more reliable marker than CYP3A4 activity for detecting pregnane X receptor-activated induction of drug-metabolizing enzymes. *Drug Metab Dispos* **38:**1605-1611

Fahmi OA and Ripp SL (2011) Evaluation of models for predicting drug-drug interactions due to induction. *Expert Opin Drug Metab Toxicol* **6:**1399-1416.

Fahmi OA, Raucy JL, Ponce E, Hassanali S and Lasker JM (2012). Utility of DPX2 cells for predicting CYP3A induction-mediated drug-drug interactions and associated structure-activity relationships. *Drug Metab Dispos* **40:**2204-2211.

FDA (2012) Guidance for Industry- Drug interaction studies- study design, data analysis, implications for dosing, and labeling recommendations (draft guidance). http://www.fda.gov/downloads/Drugs/GuidanceComplianceRegulatoryInformation/Guidance

Downloaded from dmd.aspetjournals.org at ASPET Journals on April 19, 2024

DMD Fast Forward. Published on June 12, 2014 as DOI: 10.1124/dmd.114.058602
This article has not been copyedited and formatted. The final version may differ from this version.

s/ucm292362.pdf.

Furukori H, Otani K, Yasui N, Kondo T, Kaneko S, Shimoyama R, Ohkubo T, Nagasaki T and Sugawara K (1998) Effect of carbamazepine on the single oral dose pharmacokinetics of alprazolam. *Neuropsychopharmacology* **18:**364-369.

Gibbs MA, Kunze KL, Howald WN, Thummel KE(1999) Effect of inhibitor depletion on inhibitory potency: tight binding inhibition of CYP3A by clotrimazole. Drug Metab Dispos 27:596–599.

Harris RZ, Inglis AM, Miller AK, Thompson KA, Finnerty D, Patterson S, Jorkasky DK and Freed MI (1999) Rosiglitazone has no clinically significant effect on nifedipine pharmacokinetics. *J Clin Pharmacol* **39:**1189-1194.

Inglis AM, Miller AK, Culkin KT, Finnerty D, Patterson SD, Jorkasky DK and Freed MI (2001) Lack of effect of rosiglitazone on the pharmacokinetics of oral contraceptives in healthy female volunteers. *J Clin Pharmacol* **41:**683-690.

Isoherranen N, Lutz JD, Chung SP, Hachad H, Levy RH, Ragueneau-Majlessi I (2012) Importance of multi-p450 inhibition in drug-drug interactions: evaluation of incidence, inhibition magnitude, and prediction from *in vitro* data. *Chem Res Toxicol* **25:**2285-2300.

Kanebratt KP and Andersson TB (2008) HepaRG cells as an *in vitro* model for evaluation of cytochrome P450 induction in humans. *Drug Metab Dispos* **36:**137-145.

Kato M, Chiba K, Horikawa M, Sugiyama Y (2005). The quantitative prediction of *in vivo* enzyme-induction caused by drug exposure from *in vitro* information on human hepatocytes. *Drug Metab Pharmacokinet* **20:**236-243.

Kim KA, Oh SO, Park PW and Park JY (2005) Effect of probenecid on the pharmacokinetics of carbamazepine in healthy subjects. *Eur J Clin Pharmacol* **61:**275-280.

Downloaded from dmd.aspetjournals.org at ASPET Journals on April 19, 2024

DMD Fast Forward. Published on June 12, 2014 as DOI: 10.1124/dmd.114.058602
This article has not been copyedited and formatted. The final version may differ from this version.

Kirby BJ, Collier AC, Kharasch ED, Whittington D, Thummel KE and Unadkat JD (2011) Complex drug interactions of HIV protease inhibitors 1: inactivation, induction, and inhibition of cytochrome P450 3A by ritonavir or nelfinavir. *Drug Metab Dispos* **39:**1070-1078.

Leizorovicz A, Piolat C, Boissel JP, Sanchini B and Ferry S (1984) Comparison of two long-acting forms of quinidine. *Br J Clin Pharmacol* 17:729-734.

Livak KJ and Schmittgen TD (2001) Analysis of relative gene expression data using real-time quantitative PCR and the $2^{-\Delta\Delta CT}$ method. *Methods* **25:** 402-408.

Ma JD, Nafziger AN, Rhodes G, Liu S and Bertino JS (2006) Duration of pleconaril effect on cytochrome P450 3A activity in healthy adults using the oral biomarker midazolam. *Drug Metab Dispos.* **34:**783-785.

McGinnity DF, Zhang G, Kenny JR, Hamilton GA, Otmani S, Stams KR, Haney S, Brassil P, Stresser DM and Riley RJ (2009) Evaluation of multiple *in vitro* systems for assessment of CYP3A4 induction in drug discovery: human hepatocytes, pregnane X receptor reporter gene, and Fa2N-4 and HepaRG cells. *Drug Metab Dispos* **37:**1259-1268.

Mihaly GW, Ching MS, Klejn MB, Paull J and Smallwood RA (1987) Differences in the binding of quinine and quinidine to plasma proteins. *Br J Clin Pharmacol* **24:**769-774.

Ohtsuki S, Schaefer O, Kawakami H, Inoue T, Liehner S, Saito A, Ishiguro N, Kishimoto W, Ludwig-Schwellinger E, Ebner T, et al.(2012) Simultaneous absolute protein quantification of transporters, cytochromes P450, and UDP-glucuronosyltransferases as a novel approach for the characterization of individual human liver: comparison with mRNA levels and activities. *Drug Metab Dispos* **40**:83–92.

O'Reilly RA (1982) Stereoselective interaction of sulfinpyrazone with racemic warfarin and its

Downloaded from dmd.aspetjournals.org at ASPET Journals on April 19, 2024

DMD Fast Forward. Published on June 12, 2014 as DOI: 10.1124/dmd.114.058602
This article has not been copyedited and formatted. The final version may differ from this version.

separated enantiomorphs in man. *Circulation* **65:**202-207.

Prueksaritanont T, Vega JM, Zhao J, Gagliano K, Kuznetsova O, Musser B, Amin RD, Liu L, Roadcap BA, Dilzer S, Lasseter KC and Rogers JD (2001) Interactions between simvastatin and troglitazone or pioglitazone in healthy subjects. *J Clin Pharmacol* **41:**573-581.

Ripp SL, Mills JB, Fahmi OA, Trevena KA, Liras JL, Maurer TS, de Morais SM (2006) Use of immortalized human hepatocytes to predict the magnitude of clinical drug-drug interactions caused by CYP3A4 induction. *Drug Metab Dispos* **34:**1742-1748.

Schellens JH, van der Wart JH, Brugman M and Breimer DD (1989) Influence of enzyme induction and inhibition on the oxidation of nifedipine,sparteine, mephenytoin and antipyrine in humans as assessed by a "cocktail" study design. *J Pharmacol Exp Ther.* **249:**638-645.

Selen A, Amidon GL and Welling PG (1982) Pharmacokinetics of probenecid following oral doses to human volunteers. *J Pharm Sci* **71:**1238-1242.

Shimada T, Yamazaki H, Mimura M, Inui Y, and Guengerich FP (1994) Interindividual variations in human liver cytochrome P-450 enzymes involved in the oxidation of drugs, carcinogens and toxic chemicals: studies with liver microsomes of 30 Japanese and 30 Caucasians. *J Pharmacol Exp Ther* **270:**414–423.

Shord SS, Chan LN, Camp JR, Vasquez EM, Jeong HY, Molokie RE, Baum CL and Xie H (2010) Effects of oral clotrimazole troches on the pharmacokinetics of oral and intravenous midazolam. *Br J Clin Pharmacol* **69:**160-166.

Shou M, Hayashi M, Pan Y, Xu Y, Morrissey K, Xu L, Skiles GL (2008) Modeling, prediction, and *in vitro in vivo* correlation of CYP3A4 induction. *Drug Metab Dispos* **36:**2355-2370.

Soons PA, van den Berg G, Danhof M, van Brummelen P, Jansen JB, Lamers CB and Breimer DD (1992) Influence of single- and multiple-dose omeprazole treatment on nifedipine

Downloaded from dmd.aspetjournals.org at ASPET Journals on April 19, 2024

DMD Fast Forward. Published on June 12, 2014 as DOI: 10.1124/dmd.114.058602
This article has not been copyedited and formatted. The final version may differ from this version.

pharmacokinetics and effects in healthy subjects. *Eur J Clin Pharmacol* **42:**319-324.

Wienkers LC and Heath TG (2005) Predicting in vivo drug interactions from in vitro drug discovery data. *Nat Rev Drug Discov* **4**:825-833

Williams JA, Ring BJ, Cantrell VE, Jones DR, Eckstein J, Ruterbories K, Hamman MA, Hall SD, and Wrighton SA(2002) Comparative metabolic capabilities of CYP3A4, CYP3A5, and CYP3A7. *Drug Metab Dispos* **30**:883–891

Xu Y, Zhou Y, Hayashi M, Shou M, Skiles GL (2011) Simulation of clinical drug-drug interactions from hepatocyte CYP3A4 induction data and its potential utility in trial designs. *Drug Metab Dispos* **39:**1139-1148.

Zhang JG, Ho T, Callendrello AL, Crespi CL and Stresser DM (2010). A multi-endpoint evaluation of cytochrome P450 1A2, 2B6 and 3A4 induction response in human hepatocyte cultures after treatment with β-naphthoflavone, phenobarbital and rifampicin. *Drug Metab Lett* **4:**185-194.

Downloaded from dmd.aspetjournals.org at ASPET Journals on April 19, 2024

DMD Fast Forward. Published on June 12, 2014 as DOI: 10.1124/dmd.114.058602
This article has not been copyedited and formatted. The final version may differ from this version.

Footnotes

Parts of the work were presented at the International Society for the Study of Xenobiotics (ISSX) 18th North American Regional Meeting, Oct. 14-18, 2012, Dallas, Texas and 10th international ISSX meeting, Sep. 29-Oct. 3, 2013, Toronto, Canada.

Downloaded from dmd.aspetjournals.org at ASPET Journals on April 19, 2024

DMD Fast Forward. Published on June 12, 2014 as DOI: 10.1124/dmd.114.058602
This article has not been copyedited and formatted. The final version may differ from this version.

Figure Legends

Fig. 1. Calibration curve of midazolam AUC change (%) as a function of RIS, obtained from induction data for CYP3A4 mRNA (A, based on C_{max-t}; B, based on C_{max-u}) and testosterone 6ß-hydroxylase activity (C, based on C_{max-t}; D, based on C_{max-u}) in lot 295 human hepatocytes. The RIS values were calculated based on both total and unbound C_{max}. The interacting drugs used for the curve fitting are shown in Table 3. See supplement data for lots 312 and 318.

Fig. 2. Calibration curve of midazolam AUC change (%) as a function of R_3, obtained from induction data for CYP3A4 mRNA (A, based on C_{max-t}; B, based on C_{max-u}) and testosterone 6ß-hydroxylase activity (C, based on C_{max-t}; D, based on C_{max-u}) in Lot 295 human hepatocytes. The R_3 values were calculated based on both total and unbound C_{max}. The interacting drugs used for the curve fitting are shown in Table 3. See supplement data for lots 312 and 318.

Fig. 3. Calibration curve of midazolam AUC change (%) as a function of C_{max}/EC_{50}, obtained from induction data for CYP3A4 mRNA (A, based on C_{max-t}; B, based on C_{max-u}) and testosterone 6ß-hydroxylase activity (C, based on C_{max-t}; D, based on C_{max-u}) in Lot 295 human hepatocytes. The C_{max}/EC_{50} values were calculated based on both total and unbound C_{max}. The interacting drugs used for the curve fitting are shown in Table 3. See supplement data for lots 312 and 318.

Fig. 4. Calibration curve of observed midazolam AUC change (%) as a function of AUC/F_2, obtained from induction data for CYP3A4 mRNA (A) and testosterone 6ß-hydroxylase

Downloaded from dmd.aspetjournals.org at ASPET Journals on April 19, 2024

DMD Fast Forward. Published on June 12, 2014 as DOI: 10.1124/dmd.114.058602
This article has not been copyedited and formatted. The final version may differ from this version.

activity (B) in Lot 295 human hepatocytes. The interacting drugs used for the curve fitting are shown in Table 3. See supplemental data for lots 312 and 318.

Fig. 5. Correlation analysis of observed midazolam and non-midazolam AUC change (%) and predicted AUC changed (%) from RIS (A, based on $C_{max\text{-}t}$; B, based on $C_{max\text{-}u}$), R_3 (C, based on $C_{max\text{-}t}$; D, based on $C_{max\text{-}u}$), and C_{max}/EC_{50} (E, based on $C_{max\text{-}t}$; F, based on $C_{max\text{-}u}$) derived from CYP3A4 mRNA for three lots of human hepatocytes. Solid black line represents unity. Dashed lines represent the boundary denoting predicted changes within ±20% of observed. The data points outside of these lines were considered either under- or over-predicted.

Fig. 6. Correlation analysis of observed midazolam and non-midazolam AUC change (%) and predicted AUC changed (%) from RIS (A, based on $C_{max\text{-}t}$; B, based on $C_{max\text{-}u}$), R_3 (C, based on $C_{max\text{-}t}$; D, based on $C_{max\text{-}u}$), and C_{max}/EC_{50} (E, based on $C_{max\text{-}t}$; F, based on $C_{max\text{-}u}$) derived from CYP3A4 enzyme activity for three lots of human hepatocytes. Solid black line represents unity. Dashed lines represent the boundary denoting predicted changes within ±20% of observed. The data points outside of these lines were considered either under- or over-predicted.

Fig. 7. Correlation analysis of observed midazolam and non-midazolam AUC change (%) and predicted AUC changed (%) from AUC/F_2 derived from CYP3A4 mRNA (A) and enzyme activity (B) for three lots of human hepatocytes. Solid black line represents unity. Dashed lines represent the boundary denoting predicted changes within ±20% of observed. The data points outside of these lines were considered either under- or over-

Downloaded from dmd.aspetjournals.org at ASPET Journals on April 19, 2024

DMD Fast Forward. Published on June 12, 2014 as DOI: 10.1124/dmd.114.058602
This article has not been copyedited and formatted. The final version may differ from this version.

predicted.

Fig. 8. Correlation analysis of observed midazolam and non-midazolam AUC change (%) and % of positive control response, derived from CYP3A4 mRNA and enzyme activity for three lots of human hepatocytes.

Downloaded from dmd.aspetjournals.org at ASPET Journals on April 19, 2024

TABLE 1 EC_{50}, E_{max}, F_2, and % of positive control rifampicin response (% PC) obtained with CYP3A4 mRNA expression induction data from three lots of human hepatocytes

Test Drug	Test Concentration Range (μM)	Lot 295				Lot 312				Lot 318			
		EC_{50} (μM)	E_{max} (Fold)	F_2 (μM)	% PC	EC_{50} (μM)	E_{max} (Fold)	F_2 (μM)	% PC	EC_{50} (μM)	E_{max} (Fold)	F_2 (μM)	% PC
Rifampicin	0.01-50	0.12	7.3	0.046	100	1.4	16	0.20	100	0.44	7.4	0.11	100
Phenytoin	0.23-500	14	3.6	7.9	40	13	4.6	12	23	9.5	4.1	8.3	44
Carbamazepine	0.23-500	17	4.4	13	52	27	6.4	9.3	28	4.3	14	2.5	218
Phenobarbital	0.91-2000	237	7.2	116	96	83	6.1	14	34	138	8.3	78	106
Troglitazone	0.03-20	4.4	10	0.75	139	1.0	3.7	0.48	20	5.7	5.1	3.2	59
Terbinafine	0.05-100	2.6	3.4	1.3	39	2.2	3.1	1.3	14	8.6	2.8	6.3	27
Pleconaril	0.05-100	2.9	1.4	18	6	3.4	3.0	2.7	13	6.4	1.9	11	12
Sulfinpyrazone	0.09-200	13	14	3.1	186	28	19	3.1	119	8.2	5.8	3.1	69
Probenecid	0.05-300	39	4.6	32	56	123	9.2	78	55	77	6.6	29	80
Pioglitazone	0.05-100	2.9	1.8	4.1	13	3.9	3.5	3.3	17	3.5	3.2	3.2	31
Dexamethasone	0.11-250	31	8.4	18	114	22	7.4	14	44	25	3.8	15	41
Rosiglitazone	0.05-100	8.5	4.1	3.4	47	7.8	7.5	2.7	44	10	7.3	5.0	90
Omeprazole	0.05-100	8.0	1.9	6.5	13	4.8	2.8	3.5	12	NA[1]	2.2	NA	17
Clotrimazole	0.005-10	3.3	7.8	1.6	104	2.6	6.3	1.1	36	4.1	5.3	3.5	62

Downloaded from dmd.aspetjournals.org at ASPET Journals on April 19, 2024

DMD Fast Forward. Published on June 12, 2014 as DOI: 10.1124/dmd.114.058602
This article has not been copyedited and formatted. The final version may differ from this version.

Nifedipine	0.05-100	8.0	7.7	3.2	104	13	5.7	8.8	32	6.3	3.3	4.4	33
Flumazenil	0.023-50	NI	NI	22	NA	23	2.5	25	10	NI	NI	NI	NI
Quinidine	0.11-250	11	1.5	11	7	15	6.9	8.04	31	NA	NA	NA	24
Primaquine	0.04-40	NI	NI	NI	NI	NI	NI	NI	NI	NI	NI	NI	NI
Methotrexate	0.2-20	NI	NI	NI	NI	NI	NI	NI	NI	NI	NI	NI	NI
Digoxin	0.0002-0.2	NI	NI	NI	NI	NI	NI	NI	NI	NI	NI	NI	NI

[1] - NA - not applicable; insufficient response for a reliable estimate; NI - no induction was found at the concentrations tested.

DMD Fast Forward. Published on June 12, 2014 as DOI: 10.1124/dmd.114.058602
This article has not been copyedited and formatted. The final version may differ from this version.

Downloaded from dmd.aspetjournals.org at ASPET Journals on April 19, 2024

TABLE 2 EC_{50}, E_{max}, F_2, and % of positive control rifampicin response (% PC) obtained with CYP3A4-mediated testosterone 6β-hydroxylation induction data from three lots of human hepatocytes

Test Drug	Test Concentration Range (μM)	Lot 295				Lot 312				Lot 318			
		EC_{50} (μM)	E_{max} (Fold)	F_2 (μM)	% PC) (	EC_{50} (μM)	E_{max} (Fold)	F_2 (μM)	% PC	EC_{50} (μM)	E_{max} (Fold)	F_2 (μM)	% PC
Rifampicin	0.01-50	0.18	5.9	0.011	100	1.1	8.9	0	100	0.65	3.2	0.20	100
Phenytoin	0.23-500	9.9	2.6	8.0	34	10	3.2	9.8	28	6.7	1.9	18	47
Carbamazepine	0.23-500	22	2.6	21	30	15	2.8	18	26	5.5	1.9	8.8	50
Phenobarbital	0.91-2000	153	4.0	91	63	195	4.8	117	49	106	2.0	511	52
Troglitazone	0.03-20	1.3	2.7	1.4	36	1.4	2.7	1.2	22	1.2	1.8	6.0	40
Terbinafine	0.05-100	3.2	2.9	2.9	39	4.6	3.8	2.9	35	4.8	1.6	9.3	46
Pleconaril	0.05-100	4.0	1.6	NA[1]	13	4.0	2.0	7.4	13	3.7	1.5	NA	26
Sulfinpyrazone	0.09-200	7.5	3.3	7.4	55	8.2	3.5	7.8	34	4.9	2.2	9.4	63
Probenecid	0.05-300	39	2.6	42	33	90	3.0	65	26	36	1.7	NA	35
Pioglitazone	0.05-100	2.7	2.4	3.3	24	4.2	2.5	5.2	19	2.9	1.6	NA	31
Dexamethasone	0.11-250	18	3.3	15	48	20	3.9	16	37	17	2.3	34	70
Rosiglitazone	0.05-100	7.5	3.7	5.0	57	11	6.3	6.4	67	8.0	2.9	11	98
Omeprazole	0.05-100	3.8	1.5	NA	11	2.4	1.4	NA	6	1.2	1.4	NA	23
Clotrimazole	0.005-10	1.1	3.3	0.99	47	1.0	3.1	1.0	26	NA	NA	NA	5

Downloaded from dmd.aspetjournals.org at ASPET Journals on April 19, 2024

DMD Fast Forward. Published on June 12, 2014 as DOI: 10.1124/dmd.114.058602
This article has not been copyedited and formatted. The final version may differ from this version.

Nifedipine	0.05-100	3.2	3.0	2.7	41	4.5	2.3	5.2	17	6.5	1.4	NA	20
Flumazenil	0.023-50	NI	NI	NI	NI	NA	1.4	NA	5	NI	NI	NI	NI
Quinidine	0.11-250	NI	NI	NI	NI	NI	NI	NI	NI	NI	NI	NI	NI
Primaquine	0.04-40	NI	NI	NI	NI	NI	NI	NI	NI	NI	NI	NI	NI
Methotrexate	0.2-20	NI	NI	NI	NI	NI	NI	NI	NI	NI	NI	NI	NI
Digoxin	0.0002-0.2	NI	NI	NI	NI	NI	NI	NI	NI	NI	NI	NI	NI

[1] - NA - not applicable; insufficient response for a reliable estimate; NI - no induction was found at the concentrations tested.

DMD Fast Forward. Published on June 12, 2014 as DOI: 10.1124/dmd.114.058602
This article has not been copyedited and formatted. The final version may differ from this version.

Downloaded from dmd.aspetjournals.org at ASPET Journals on April 19, 2024

TABLE 3 Clinical pharmacokinetic and drug-drug interaction data

Category of Clinical	Interacting Drug	C_{max-t} (μM)	C_{max-u} (μM)	AUC (h. μM)	Victim Drug	Observed AUC Change	References
Strong, ≥80% decrease in AUC	Rifampicin*[1]	15	3.6	34	midazolam	98	Backman et al., 1998; Kanebratt and Anderson, 2008
	Rifampicin*	11	2.7	34	midazolam	95	Eap et al., 2004
	Rifampicin*	10	2.5	34	midazolam	97	Fahmi et al., 2012; Backman et al.,1996[a]
	Rifampicin*	6.5	1.6	34	midazolam	86	Adams et al.,2005
	Phenytoin*	29	7.3	468	midazolam	94	Backman et al., 1996[b]; Kanebratt and Anderson, 2008
	Carbamazepine*	21	5.3	1248	midazolam	94	Backman et al., 1996[b]; Kanebratt and Anderson, 2008
	Carbamazepine	25	6.1	1248	alprazolam	58	Furukori et al.,1998
Moderate, 50-80% decrease in AUC	Phenobarbital	56	28	1497	nifedipine	61	Schellens et al.,1989, Kanebratt and Anderson, 2008
	Troglitazone	3.1	0.031	24	simvastatin	38	Fahmi et al., 2012, Prueksaritanont et al, 2001,Kanebratt and Anderson, 2008
	Troglitazone*	6.3	0.063	50	midazolam	67	Fahmi et al., 2012
Weak, 20-50% decrease in AUC	Terbinafine*	2.4	0.024	16	midazolam	25	Ahonen, et al.,1995
	Pleconaril*	3.0	0.030	42	midazolam	35	Ma, et al., 2006; Fahmi and Ripp, 2010
	Pioglitazone	4.5	0.045	44	simvastatin	-1	Prueksaritanont et al., 2001; Fahmi and Ripp, 2011
	Pioglitazone*	2.8	0.028	44	midazolam	26	Fahmi et al., 2012

Downloaded from dmd.aspetjournals.org at ASPET Journals on April 19, 2024

DMD Fast Forward. Published on June 12, 2014 as DOI: 10.1124/dmd.114.058602
This article has not been copyedited and formatted. The final version may differ from this version.

	Sulfinpyrazone	48	0.96	287	R-warfarin	22	O'Reilly, 1982; Kanebratt and Andersson,2008
	Probenecid	244	24	2705	carbamazepine	20	Kim et al.,2005; Selen et al., 1982
Clinical non-inducer	Dexamethasone	0.021	0.0054	0.29	triazolam	19	Fahmi et al., 2012, Kanebratt and Andersson, 2008
	Nifedipine*	0.40	0.020	0.87	midazolam	4	Fahmi et al., 2012, Kanebratt and Andersson, 2008
	Rosiglitazone	1.7	0.0033	8.2	nifedipine	12	Fahmi et al., 2012, Harris et al.,1999; Fahmi and Ripp, 2011
	Rosiglitazone	1.4	0.0028	8.2	ethinylestradiol	-1	Inglis A et al., 2001; Fahmi and Ripp, 2011
	Omeprazole	0.74	0.037	1.1	nifedipine	-25	Soons, et al., 1992; Kanebratt and Andersson, 2008
	Clotrimazole*	0.0074	0.0001	NA[2]	midazolam	9.7	Shord et al., 2010
	Flumazenil	0.0010	0.0005	0.050	midazolam	-2	Fahmi et al., 2012
	Quinidine	3.3	0.41	42	NA	0	Mihaly et al.,1987; Leizorovicz et al., 1984

[1] – Interacting drugs marked with an asterisk were used for preparation of calibration curves. [2] – NA, clinical induction interaction data not available.

Downloaded from dmd.aspetjournals.org at ASPET Journals on April 19, 2024

DMD Fast Forward. Published on June 12, 2014 as DOI: 10.1124/dmd.114.058602
This article has not been copyedited and formatted. The final version may differ from this version.

DMD Fast Forward. Published on June 12, 2014 as DOI: 10.1124/dmd.114.058602
This article has not been copyedited and formatted. The final version may differ from this version.

TABLE 4 Summary of cut-off values, confidence interval (CI), and correlation co-efficients (R^2) of calibration curves for RIS, R_3, $C_{max}/EC_{50,}$ and AUC/F_2

Hepatocyte Lot No	Parameters	RIS		R_3		C_{max}/EC_{50}		AUC/F_2
		C_{max-t}	C_{max-u}	C_{max-t}	C_{max-u}	C_{max-t}	C_{max-u}	
mRNA Data								
	Cut-off value	**0.74**	**0.017**	**0.57**	**0.98**	**0.94**	**0.0088**	**6.2**
Lot 295	**95% CI**	0.54	0.013	0.20	0.029	0.079	0.00084	7.0
	R^2	0.91	0.97	0.91	0.98	0.97	0.995	0.94
	Cut-off value	**1.32**	**0.019**	**0.44**	**0.98**	**0.23**	**0.0056**	**12**
Lot 312	**95% CI**	0.28	0.0093	0.062	0.037	0.46	0.0028	3.4
	R^2	0.97	0.99	0.97	0.98	0.84	0.99	0.97
	Cut-off value	**0.62**	**0.011**	**0.62**	**0.99**	**0.33**	**0.0038**	**2.3**
Lot 318	**95% CI**	0.35	0.011	0.18	0.014	0.21	0.0021	2.6
	R^2	0.96	0.96	0.97	0.97	0.97	0.97	0.95
Activity Data								
	Cut-off value	**0.60**	**0.017**	**0.63**	**0.98**	**0.62**	**0.0069**	**8.8**
Lot 295	**95% CI**	0.63	0.011	0.28	0.026	0.43	0.0034	5.4
	R^2	0.87	0.97	0.87	0.98	0.88	0.98	0.98
	Cut-off value	**0.84**	**0.013**	**0.56**	**0.99**	**0.58**	**0.005**	**4.4**
Lot 312	**95% CI**	0.37	0.0069	0.13	0.023	0.15	0.0025	2.7
	R^2	0.93	0.98	0.93	0.98	0.97	0.99	0.97
	Cut-off value	**0.57**	**0.0078**	**0.65**	**0.995**	**0.53**	**0.0052**	**1.0**
Lot 318	**95% CI**	0.18	0.0039	0.084	0.020	0.34	0.0025	3.2
	R^2	0.97	0.99	0.97	0.98	0.96	0.99	0.78

RIS, R_3, C_{max}/EC_{50} were calculated using both C_{max-t} and C_{max-u}. Cut-off values for RIS, R_3, C_{max}/EC_{50} and AUC/F_2 were defined as that corresponding to 20% predicted AUC change.

Downloaded from dmd.aspetjournals.org at ASPET Journals on April 19, 2024

TABLE 5 R_3 values calculated based on total and unbound C_{max} for induction response of CYP3A4 mRNA and enzyme activity in three lots of human hepatocytes

Category of Clinical Inducer	Interacting Drug	Lot 295				Lot 312				Lot 318			
		$R_{3\text{-}Cmax\text{-}t}$		$R_{3\text{-}Cmax\text{-}u}$		$R_{3\text{-}Cmax\text{-}t}$		$R_{3\text{-}Cmax\text{-}u}$		$R_{3\text{-}Cmax\text{-}t}$		$R_{3\text{-}Cmax\text{-}u}$	
		mRNA	Activity	mRNA	Activity	mRNA	Activity	mRNA	Activity	mRNA	Activity	mRNA	Activity
Strong, ≥80% decrease in AUC	Rifampicin	0.12	0.15	0.12	0.15	0.065	0.11	0.080	0.13	0.12	0.25	0.13	0.27
	Rifampicin	0.12	0.15	0.12	0.15	0.067	0.11	0.087	0.14	0.12	0.25	0.13	0.28
	Rifampicin	0.12	0.15	0.13	0.15	0.067	0.11	0.089	0.14	0.12	0.25	0.14	0.29
	Rifampicin	0.12	0.15	0.13	0.16	0.071	0.12	0.10	0.16	0.13	0.26	0.15	0.31
	Phenytoin	0.29	0.34	0.45	0.48	0.24	0.30	0.38	0.43	0.25	0.40	0.36	0.51
	Carbamazepine	0.29	0.44	0.50	0.67	0.26	0.38	0.49	0.58	0.082	0.40	0.12	0.52
	Carbamazepine	0.28	0.42	0.47	0.64	0.25	0.37	0.46	0.55	0.080	0.39	0.11	0.50
Moderate, 50-80% decrease in AUC	Phenobarbital	0.42	0.48	0.57	0.62	0.29	0.48	0.40	0.63	0.29	0.59	0.42	0.71
	Troglitazone	0.20	0.34	**0.93**[1]	**0.94**	0.27	0.34	**0.90**	**0.94**	0.36	0.44	**0.97**	**0.96**
	Troglitazone	0.15	0.31	0.88	0.89	0.24	0.31	0.83	0.89	0.27	0.40	**0.95**	**0.92**
Weak, 20-50% decrease	Terbinafine	0.38	0.45	**0.97**	**0.98**	0.38	0.43	**0.97**	**0.98**	0.62	0.65	**0.99**	**0.99**
	Pleconaril	0.59	0.59	**0.99**	**0.99**	0.42	0.54	**0.97**	**0.99**	0.63	0.60	**0.99**	**0.99**
	Pioglitazone	0.47	0.40	**0.97**	**0.96**	0.35	0.44	**0.96**	**0.97**	0.36	0.51	**0.96**	**0.98**

Downloaded from dmd.aspetjournals.org at ASPET Journals on April 19, 2024

DMD Fast Forward. Published on June 12, 2014 as DOI: 10.1124/dmd.114.058602
This article has not been copyedited and formatted. The final version may differ from this version.

in AUC	Pioglitazone	0.52	0.45	**0.98**	**0.98**	0.41	0.50	**0.98**	**0.98**	0.42	0.56	**0.98**	**0.98**
	Sulfinpyrazone	0.080	0.26	0.51	0.73	0.078	0.25	0.61	0.73	0.17	0.34	0.62	0.74
	Probenecid	0.20	0.31	0.36	0.50	0.14	0.31	0.40	0.61	0.17	0.41	0.39	0.60
Clinical non-inducer	Dexamethasone	0.99	1.00	1.0	1.0	0.99	1.0	1.0	1.0	1.0	1.0	1.0	1.0
	Nifedipine	**0.73**	**0.75**	0.98	0.98	**0.85**	**0.84**	0.99	1.0	**0.76**	0.93	0.98	1.0
	Rosiglitazone	**0.60**	**0.60**	1.0	1.0	**0.43**	**0.54**	1.0	1.0	**0.50**	**0.67**	1.0	1.0
	Rosiglitazone	**0.64**	**0.63**	1.0	1.0	**0.47**	**0.58**	1.0	1.0	**0.54**	**0.70**	1.0	1.0
	Omeprazole	**0.86**	**0.81**	0.99	0.99	**0.73**	0.75	0.98	NA	NA	0.64	NA	1.0
	Clotrimazole	0.98	0.98	1.0	1.0	0.98	0.98	1.0	0.99	0.99	NA	1.0	NA
	Flumazenil	NA	NA	NA	NA	1.0	NA	1.0	NA	NA	NA	NA	NA
	Quinidine	**0.75**	NA	0.95	NA	**0.44**	NA	**0.84**	NA	NA	NA	NA	NA

[1]- Values in bold were either over- or under-predicted based on the 0.9 cut-off value provided in the 2012 FDA draft guidance.

DMD Fast Forward. Published on June 12, 2014 as DOI: 10.1124/dmd.114.058602
This article has not been copyedited and formatted. The final version may differ from this version.

Downloaded from dmd.aspetjournals.org at ASPET Journals on April 19, 2024

DMD Fast Forward. Published on June 12, 2014 as DOI: 10.1124/dmd.114.058602
This article has not been copyedited and formatted. The final version may differ from this version.

TABLE 6 Accuracy and bias in the prediction of clinical CYP3A induction of midazolam and non-midazolam CYP3A substrates using the calibration-curve based approaches

Methods	Midazolam as a victim drug		Non-midazolam as a victim drug	
	GMFE	**RMSE**	**GMFE**	**RMSE**
Based on Total Cmax and mRNA Data				
RIS	1.78	0.120	2.25	0.394
R_3	1.75	0.115	2.33	0.396
C_{max}/EC_{50}	1.73	0.137	2.10	0.414
Based on Total C_{max} with Activity Data				
RIS	1.78	0.141	1.95	0.391
R_3	1.79	0.138	2.02	0.398
C_{max}/EC_{50}	1.82	0.126	2.50	0.469
Based on Unbound C_{max} with mRNA Data				
RIS	1.40	0.087	2.42	0.405
R_3	1.34	0.077	2.74	0.412
C_{max}/EC_{50}	1.34	0.065	2.65	0.434
Based on Unbound C_{max} with Activity Data				
RIS	1.37	0.071	2.32	0.409
R_3	1.34	0.071	2.78	0.415
C_{max}/EC_{50}	1.35	0.062	2.30	0.399
Based on AUC/F_2				
mRNA	1.70	0.105	1.82	0.326
Activity	1.76	0.117	1.67	0.315

The predicted fold changes in AUC from all three hepatocyte lots were used in the calculations.

Downloaded from dmd.aspetjournals.org at ASPET Journals on April 19, 2024

DMD Fast Forward. Published on June 12, 2014 as DOI: 10.1124/dmd.114.058602
This article has not been copyedited and formatted. The final version may differ from this version.

Figure 1

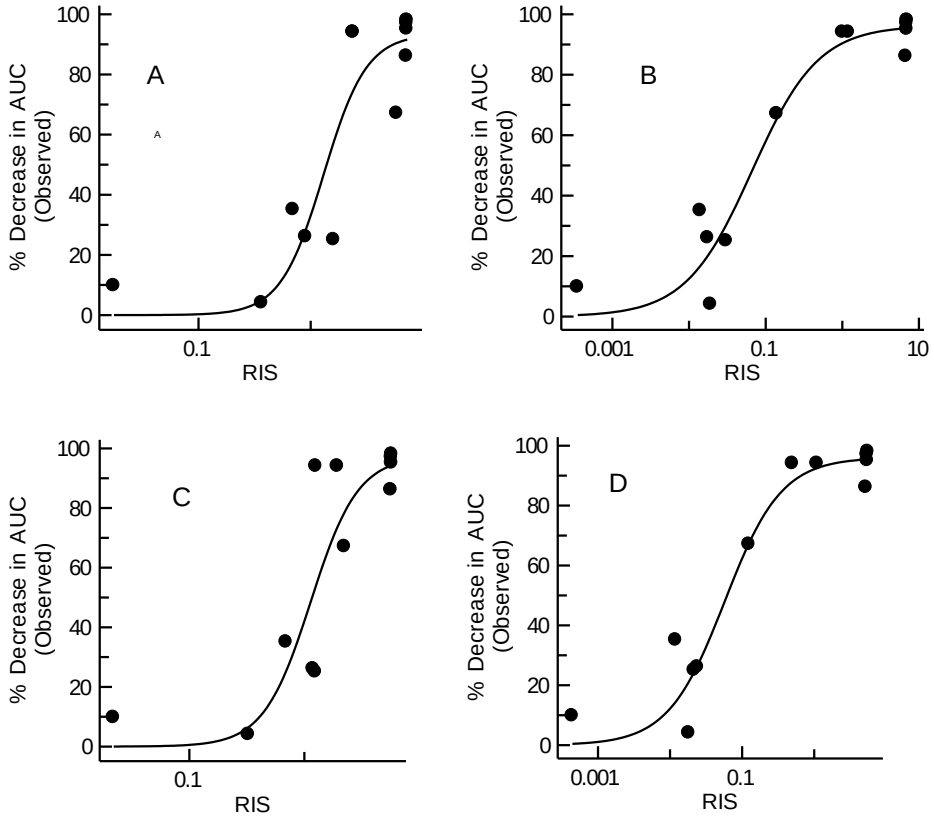

Downloaded from dmd.aspetjournals.org at ASPET Journals on April 19, 2024

DMD Fast Forward. Published on June 12, 2014 as DOI: 10.1124/dmd.114.058602
This article has not been copyedited and formatted. The final version may differ from this version.

Figure 2

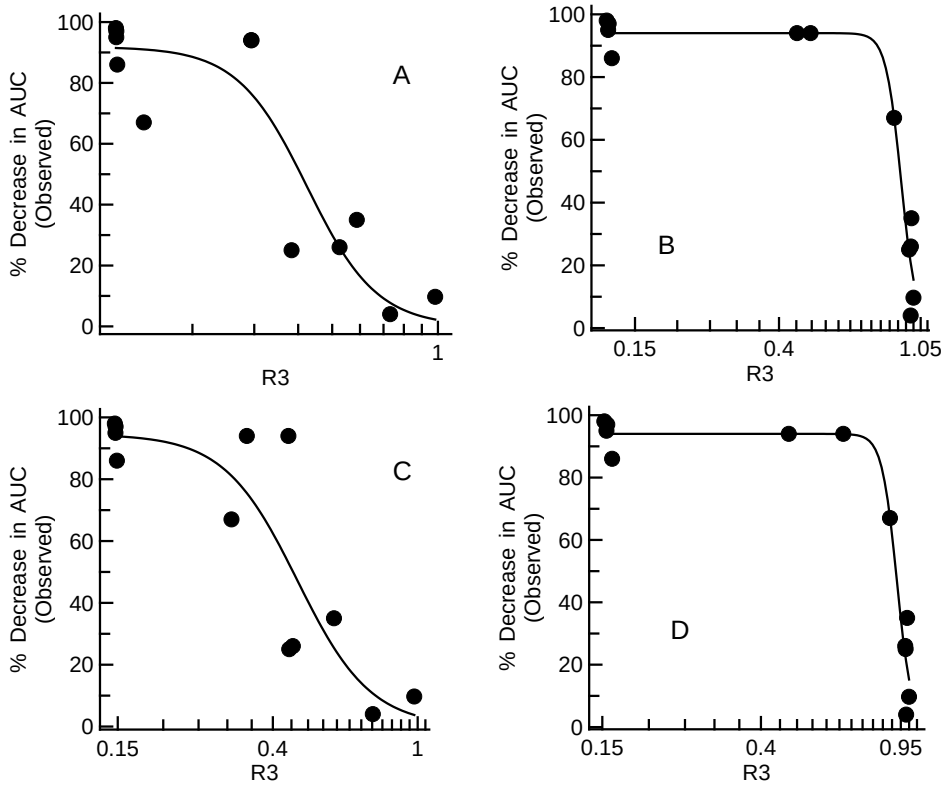

Downloaded from dmd.aspetjournals.org at ASPET Journals on April 19, 2024

DMD Fast Forward. Published on June 12, 2014 as DOI: 10.1124/dmd.114.058602
This article has not been copyedited and formatted. The final version may differ from this version.

Figure 3

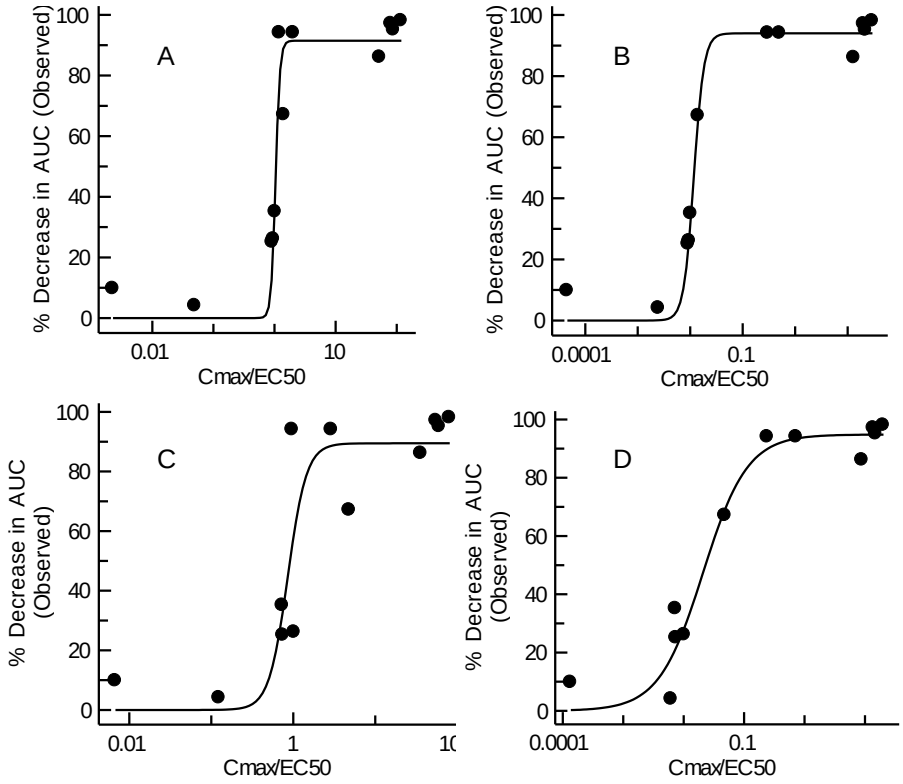

Downloaded from dmd.aspetjournals.org at ASPET Journals on April 19, 2024

DMD Fast Forward. Published on June 12, 2014 as DOI: 10.1124/dmd.114.058602
This article has not been copyedited and formatted. The final version may differ from this version.

Figure 4

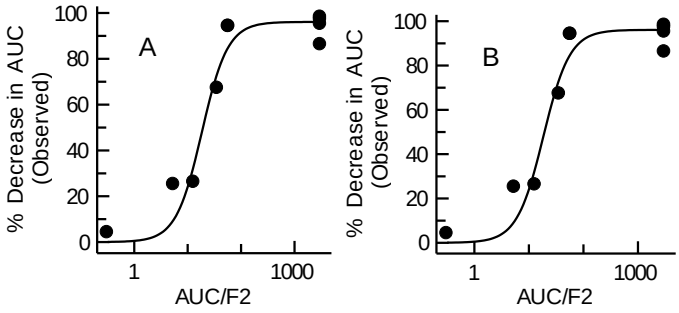

Downloaded from dmd.aspetjournals.org at ASPET Journals on April 19, 2024

DMD Fast Forward. Published on June 12, 2014 as DOI: 10.1124/dmd.114.058602
This article has not been copyedited and formatted. The final version may differ from this version.

Figure 5

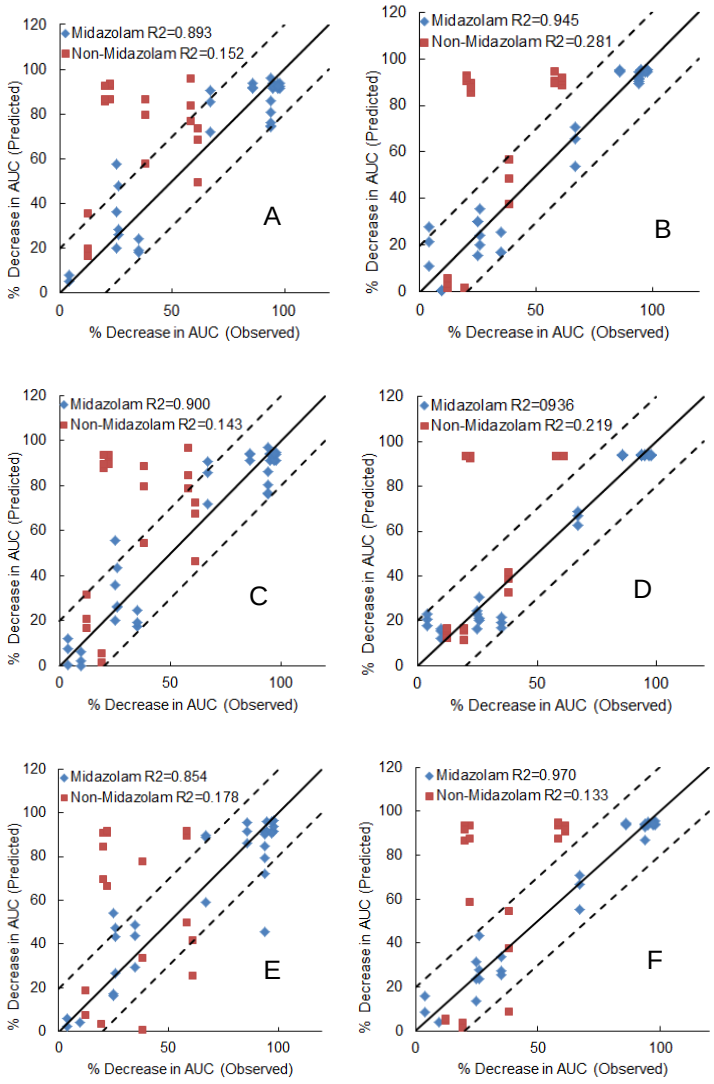

Downloaded from dmd.aspetjournals.org at ASPET Journals on April 19, 2024

DMD Fast Forward. Published on June 12, 2014 as DOI: 10.1124/dmd.114.058602
This article has not been copyedited and formatted. The final version may differ from this version.

Figure 6

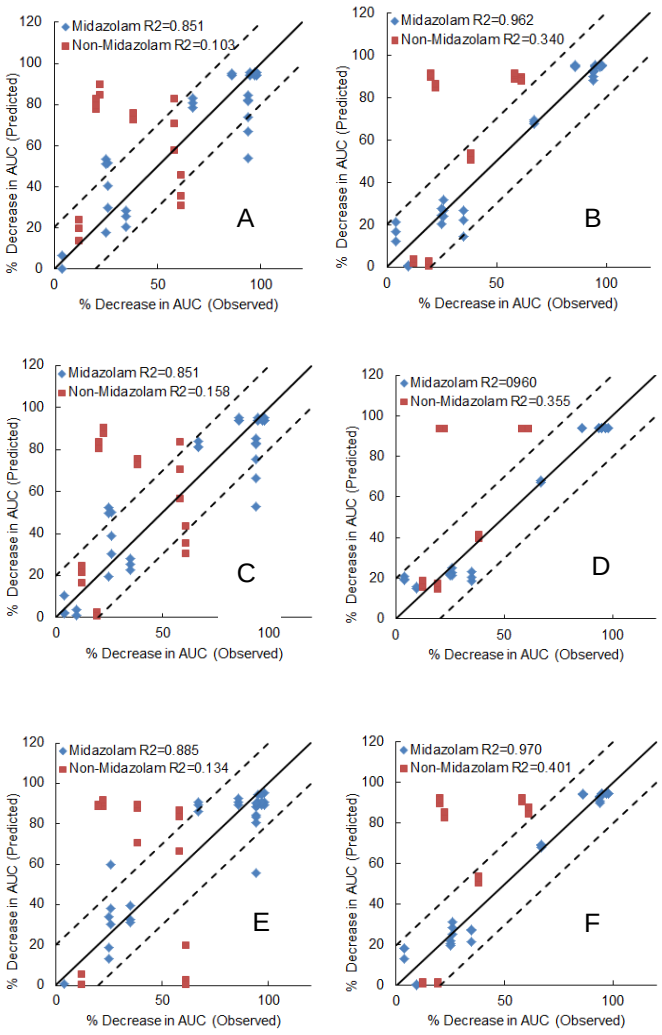

Downloaded from dmd.aspetjournals.org at ASPET Journals on April 19, 2024

DMD Fast Forward. Published on June 12, 2014 as DOI: 10.1124/dmd.114.058602
This article has not been copyedited and formatted. The final version may differ from this version.

Figure 7

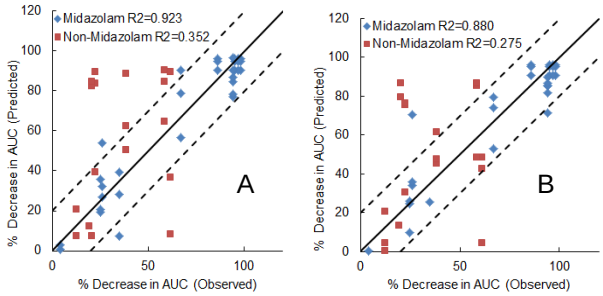

Downloaded from dmd.aspetjournals.org at ASPET Journals on April 19, 2024

DMD Fast Forward. Published on June 12, 2014 as DOI: 10.1124/dmd.114.058602
This article has not been copyedited and formatted. The final version may differ from this version.

Figure 8

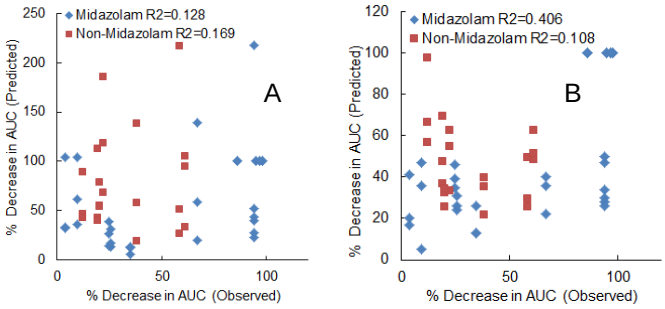

Downloaded from dmd.aspetjournals.org at ASPET Journals on April 19, 2024